Trends in Microbiology

CellPress OPEN ACCESS

Review

Substrate recruitment mechanism by gram-negative type III, IV, and VI bacterial injectisomes

Amit Meir [1,3,*] Kévin Macé, [1,4] Yogesh Vegunta, [1,4] Sunanda M. Williams, [1,4] and Gabriel Waksman [1,2,*]

Bacteria use a wide arsenal of macromolecular substrates (DNA and proteins) to interact with or infect prokaryotic and eukaryotic cells. To do so, they utilize substrate-injecting secretion systems or injectisomes. However, prior to secretion, substrates must be recruited to specialized recruitment platforms and then handed over to the secretion apparatus for secretion. In this review, we provide an update on recent advances in substrate recruitment and delivery by gram-negative bacterial recruitment platforms associated with Type III, IV, and VI secretion systems.

Introduction

Many bacteria use secretion systems to inject macromolecules such as DNAs, proteins, or other macromolecular substrates into bacterial or eukaryotic cell targets [1]. Secretion systems play pivotal roles in infectious diseases. Indeed, within gram-negative bacteria, three types of systems, namely type III (T3SS), type IV (T4SS), and type VI (T6SS) secretion systems, play essential roles in pathogenicity. Here, we propose to refer to these substrate-injecting systems as 'injectisomes', a term initially applied to only the T3SS but which we believe is suitable for other substrate-injecting machines such as T4SS and T6SS [2]. These machines are all embedded in both the inner and outer membranes and substrates are generally secreted in a one-step mechanism, where the substrate enters the double-membrane spanning secretion machinery from the cytosolic side and exits the machinery directly outside the cell without any periplasmic intermediate location [3]. Bacterial secretion systems are of great medical importance for their roles in the spread of mobile genetic elements (T4SS), such as plasmids carrying antibiotic resistance genes, or in the translocation of effector proteins that interfere with host-cell processes, thereby causing pathogenicity (T3SS, T4SS, and T6SS). All systems require a substrate recruitment platform that captures effector proteins or DNAs from the bacterial interior and delivers them to the secretion channel so they could be translocated into either another bacterium of the same species, a competitor species, or a eukaryotic host. Substrate recruitment platforms are essential for secretion system function and hence for bacterial survival and virulence.

Substrate recruitment platform capabilities are astonishingly diverse: while some substrate recruitment platforms capture a single substrate, others have evolved to capture hundreds. While some recruit uniquely proteinaceous substrates, others bind both nucleic acids and proteins or complexes of both. Substrate recruitment platforms are also diverse in their composition and architecture and vary in their mode of integration within the secretion system. Here we review recent progress made in the field of substrate recruitment mechanisms in gram-negative bacterial injectisomes, namely T3SS, T4SS, and T6SS. We first provide a brief introduction for each of these injectisomes. We next describe the nature and diversity of the substrates they inject. Since secretion requires prior binding of these substrates to specialized recruitment platforms, we then address the issue of whether injectisome substrates have defined secretion signal (SS)

Highlights

Bacterial injectisomes are crucial nanomachines responsible for the direct secretion into host cells of a variety of substrates, ranging from proteins to DNAs.

Prior to being injected, these substrates must be recruited and sometimes processed by large complexes called substrate recruitment platforms.

These platforms are characterized by:

their ability to bind effectors and effector/chaperone complexes;

their ability to target the substrates to the injectisome channel for subsequent secretion;

their diversity and complexity, some made of one component, others forming large complexes;

their diverse modes of action, some requiring an ATPase, others where the core components of the injectisome act as the payload carrier.

[1]Institute of Structural and Molecular Biology, Birkbeck and UCL, Malet Street, London WC1E 7HX, UK
[2]Institute of Structural and Molecular Biology, University College London, Gower Street, London WC1E 6BT, UK
[3]Current address: MRC Centre for Virus Research, School of Infection and Immunity, University of Glasgow, Glasgow, UK
[4]These authors contributed equally to this work

*Correspondence:
Amit.Meir@glasgow.ac.uk (A. Meir),
g.waksman@bbk.ac.uk;
g.waksman@ucl.ac.uk (G. Waksman).

sequences and next describe their cognate recruitment platforms, eventually focusing on what is known about the molecular and structural basis of substrate–platform interaction. Finally, we place the various recruitment platforms within the context of the secretion machineries, outlining mode of action, regulation, and secretion path when known.

T3SS

Pathogenic and symbiotic bacteria deploy T3SSs to facilitate communication with their environment, other bacteria, animals, or plants [4]. There are two types of T3SSs: virulent T3SSs (vT3SS), used by gram-negative bacteria for pathogenesis, and flagellar T3SSs (fT3SS), used by all bacteria for motility [5–7]. In this review, we focus on vT3SSs. vT3SS components and substrates are usually encoded in gene clusters commonly called pathogenicity islands (Figure S1A in the supplemental information online). Pathogens such as *Salmonella*, *Yersinia*, *Shigella, EPEC/EHEC*, *Pseudomonas*, etc., utilize vT3SSs to inject bacterial proteins (effectors) into hosts cytoplasm, where they interfere with a variety of physiological processes [8–11]. The vT3SS is made of multiple proteins assembling into several large substructures: (i) the needle complex (NC), which includes the basal body (BB), the inner rod, and the needle; (ii) the export apparatus (EA); (iii) the sorting complex (SC); (iv) the tip/filament; and (v) the translocation pore (or translocon) (Figure 1A). vT3SS assembly occurs in two stages: the SEC-dependent pathway assembles the BB and EA, whereas the resulting BB/EA complex assembles the inner rod and the needle, which together with tip/filament and translocon form a conduit through which effectors enter the host [4,6,12,13].

Diversity and nature of substrates

vT3SS substrates are classified into early (inner-rod and needle), middle (translocator), and late (effector) substrates. In this review, when naming vT3SS proteins, we use the unified 'Sct' nomenclature. Substrate secretion follows a strict secretion hierarchy [4,6,9,11]. Firstly, early substrates SctI (inner rod) and SctF (needle) are secreted through the BB to form the NC, which acts as a secretion channel; then, once a defined length of the needle is reached, the middle substrate tip/filament protein SctA is secreted to cap the needle, followed by secretion of translocator proteins SctB and SctE, which form the translocon (the pore through which effectors enter the host). Following translocon assembly, secretion switches to late substrate effectors classified into class-IA and class-IB substrates, depending on the type of class-I chaperones they bind to [4,6,9,12,14].

Definition and description of SSs/sequences

SSs are essential sequences for substrate targeting to the secretion apparatus [4,6]. All vT3SS substrates contain SSs embedded within the N-terminal ~20-amino acid region [15]. SSs lack conserved amino acid sequence and therefore are not characterized by a defined structural scaffold [4,6,15]. Middle substrates (translocator proteins) additionally contain one or two translocator-specific SSs termed 'translocation signal (TS)' [8,16]. Finally, all substrates contain a chaperone-binding domain (CBD), a ~100-amino acid domain with which they bind to cognate chaperones [9,15,17].

T3SS chaperones play essential roles in substrate recruitment. They are small, acidic, dimeric proteins that contain hydrophobic surfaces for binding partially unfolded substrates (Figure 1B) [9,17–19]. Chaperones, based on substrate specificity, belong to three classes (Figure 1B): (i) class-III chaperones (all heterodimeric in the substrate-bound state), which bind early substrate needle proteins; (ii) class-II chaperones (either monomeric or dimeric in the substrate-bound state), which bind middle substrate translocator proteins; and (iii) class-IA and IB chaperones (all homodimeric in the substrate-bound state), which bind late substrate effectors, class-IA

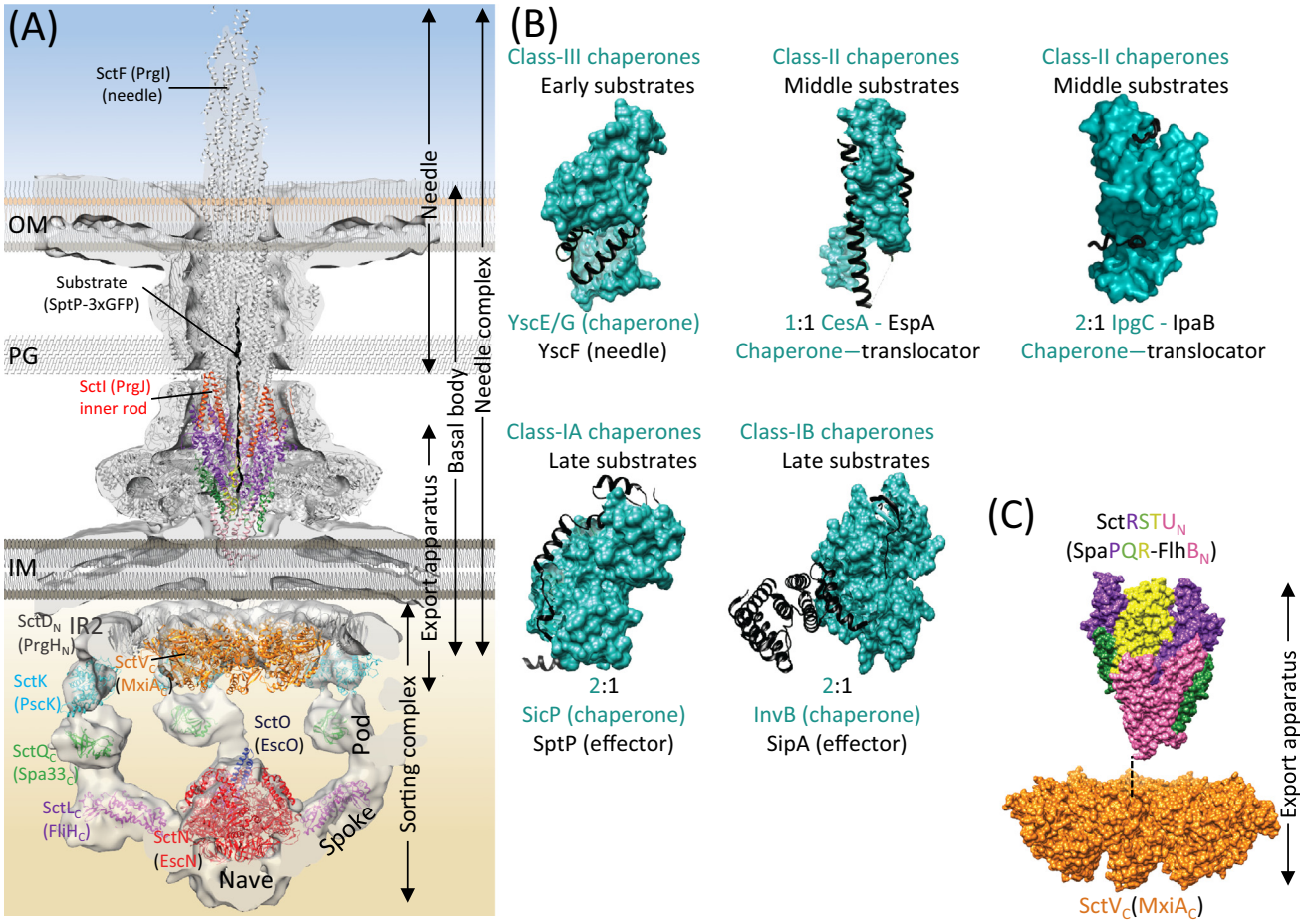

Figure 1. Type III secretion system (T3SS): machinery, substrates, and export apparatus. (A) Cryo-electron tomography structure (EMDB_8544) of *Salmonella* SPI-1 T3SS (σ 2.9), docked with X-ray and cryo-electron microscopy structures of homologs. Sources for coordinates and maps are: needle complex with export apparatus (EA) and trapped substrate (PDB_7AH9), IR2 made of SctD$_N$/PrgH$_N$ (PDB_3J1W), SctU$_N$/FlhB$_N$ (PDB_6S3L), SctV$_C$/MxiA$_C$ (PDB_4A5P), SctN-SctO/EscN-EscO (PDB_6NJP), SctQ$_C$/Spa33$_C$ (PDB_4TT9), SctL$_C$/FliH$_C$ (PDB_5B0O), and SctK/PscK (PDB_6UIE) [10,22,24,106,107]. Proteins are shown as ribbon color-coded as in Figure S1A (see the supplemental information online). The structure of the EA (SctRSTUV) is as in (C). The unfolded substrate SptP-3xGFP is indicated. (B) Representative examples of chaperone–substrate complex structures. Top row from left to right: class III YscE/G-YscF (PDB_2P58), class II CesA-EspA (PDB_1XOU), and class II IpgC-IpaB (PDB_3GZ1). Bottom row from left to right: class IA SicP-SptP (PDB_1JYO) and class IB InvB-SipA (PDB_2FM8). Chaperones are in light sea green surface representation, while substrates are in black ribbon. The stoichiometry is indicated for each complex [9,17,19,108,109]. (C) Composite model of a vT3SS EA based on the EA part of *Salmonella* SPI-1 structure (SctRST/SpaPQR; PDB_7AH9) to which the structure of SctU$_N$/FlhB$_N$ from the flagella SctRSTU$_N$/FliPQR-FlhB$_N$ structure (PDB_6S3L) was added. The SctV$_C$/MxiA$_C$ is shown underneath. SctRSTU$_N$ and SctV$_C$ are located on opposite sides of the inner membrane (IM). The connecting structure between the two (represented by a dashed line) is not known. The stoichiometry of EA components SctRSTUV is 5:4:1:1:9 [24,25,106,107]. All proteins are shown in surface representation color-coded as in indicated in labeling. Abbreviations: OM, outer membrane; IM, inner membrane; PG, peptidoglycan.

being able to interact with only one effector and class-IB chaperones being able to bind multiple substrates [4,6,9,17,18,20].

Class-IA and -IB chaperones bind to CBDs and maintain effectors in a partially unfolded secretion-competent state [9,15]. Indeed, multiple structures of class-IA or -IB chaperones bound to effector revealed that the latter wraps around both subunits of the chaperone homodimer in an extended, nonglobular state but retaining secondary structures (Figure 1B) [17,18]. However, in the case of the InvB(class-IB)-SipA complex, the effector, also partially unfolded, interacts with only one molecule of the chaperone homodimer (Figure 1B) [9]. In class II chaperone-middle

substrate complexes, the substrate's CBD (an elongated coiled-coil) forms a 1:1 heterodimeric complex with a chaperone's extended groove (Figure 1B), thereby preventing premature polymerization of middle substrates in the bacterial cytoplasm and facilitating their assembly upon secretion to the bacterial surface [19,20]. Class-III chaperones interact with the C terminus of their substrates, which prevents their polymerization (Figure 1B) [18].

Definition and description of the substrate recruitment platform and its location within the T3SS

In the T3SS field, the recruitment platform for substrates is the SC (Figure 1A) [21]. Recent cryo-electron tomography (cryo-ET) studies of *Salmonella* and *Shigella* T3SSs have revealed that the SC is a cage-like cytoplasmic structure with sixfold symmetry (Figure 1A) [13,22,23]. The SC cage has been described as a six-pod structure connected to a central nave by six spokes. In *Salmonella*, each pod is made of a copy of each of SpaO (SctQ), OrgA (SctK), and the N-terminal domain of OrgB (SctL) (Figure 1A). Each spoke is made of the C-terminal domain of OrgB, while the nave is made of the ATPase complex, which comprises InvC (SctN) and InvI (SctO) (Figure 1A). The SC is located under the NC via interactions between OrgA and the cytoplasmic inner ring 2 (IR2), an NC ring made of the N-terminal domain of PrgH (SctD) (Figure 1A).

Cryo-electron microscopy (cryo-EM) structure of the EPEC ATPase complex EscN-EscO (SctN-SctO) revealed a homo-hexameric assembly in which EscN monomers oligomerize through their N-terminal domains (Figure 1A) [10]. Their C-terminal domains form a pore and are suggested to interact with chaperone–substrate complexes. SctN family ATPases interact with accessory subunit EscO (SctO) (Figure 1A). EscO is a coiled-coil protein that, through its N and C termini, partly locates inside the C-terminal pore of EscN. EscN-EscO interaction is essential for catalysis [10]. On the inner membrane (IM) side of the SC and within the IR2 ring lies a 9-mer oligomeric structure composed of SctV, an essential component of the EA. Its cytoplasmic C-terminal domain tops the SC cage, while its trans-membrane N-terminal domain anchors it to the IM (Figure 1A) [13,22]. The EA plays an essential role in secretion as all substrates must pass through it. In addition to SctV, the EA is composed of SctRSTU that form a conical shape structure embedded in the IM but protruding into the periplasm (Figure 1A,C) [13,24,25].

Interactions between substrates and recruitment platforms

All chaperone–substrate complexes are first recruited to the ATPase complex and the interaction is predominantly with the chaperone (Figure 2, step 1), additional interactions being sometimes observed with SSs and TSs [15,16,19,20]. Although there is no structure of a complex between ATPase and chaperone, it is known that the C-terminal region of the ATPase [for example, residue 377–393 of SsaN (a SctN family ATPase)] is involved as well as multiple sites on the chaperone. Overall, ATPase–chaperone interaction interfaces are conserved [26].

Following recruitment to the ATPase, nucleotide binding and hydrolysis by the ATPase appear to destabilize the chaperone–substrate complex, leading to either total or partial release of the substrate from the chaperone and also its unfolding [14]. Based on the hexameric organization of EscN, the different functional states of its catalytic sites, and the relative orientations of EscO, a rotary catalytic mechanism generating torque, analogous to F_1/V_1-ATPases, has been proposed for T3SS ATPases [10].

Next, released or partially released substrates are handed over to the EA via interaction with EA protein SctV (Figure 2, step 2). Recent studies of SctV protein interaction with chaperone–substrate complexes have highlighted the ability of SctV to interact with both the substrate and the chaperone [27]. SctV acts as an entry portal for substrates while also serving as a channel for secreting substrates (Figure 2, step 3) [7,13,24]. Hand-over of substrates from the ATPase complex to the EA SctV may be facilitated by SctO, by bringing SctN closer to and interacting with SctV

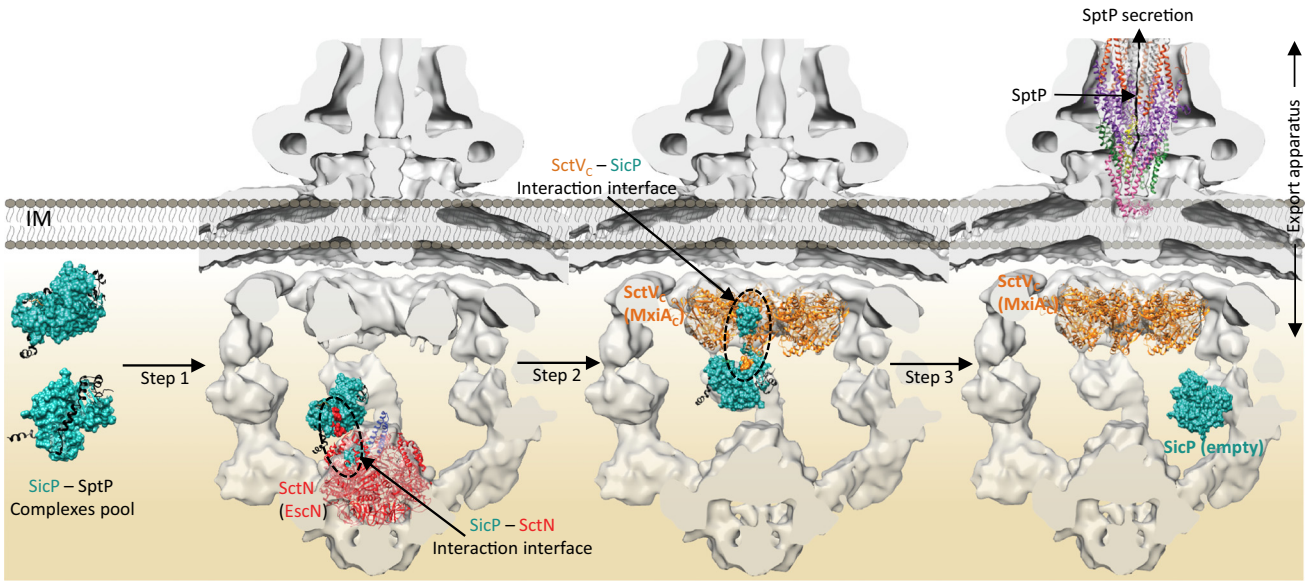

Figure 2. Mechanism of substrate recruitment by type III secretion system (T3SS). In all steps, the sorting complex (SC) cryo-electron tomography structure (EMDB_8544) of *Salmonella* SPI-1 T3SS is shown as in Figure 1A. The chaperone–substrate complex exemplified by SicP-SptP is shown as in Figure 1B. Interaction surfaces between the chaperone SicP and the ATPase SctN/EscN or between SicP and export apparatus (EA) component SctV$_C$/MxiA$_C$ are shown as surfaces color-coded using the color of the interaction partner. For example, the ATPase SctN/EscN is in red ribbon but its interaction surfaces with SicP are shown in light sea green surface. Step 1: binding of a SicP-SptP complex from SicP-SptP pool to the ATPase complex SctNO/EscNO (red and blue, respectively; SctO/EscO not labeled for clarity). Step 2: handing over of SicP-SptP to the EA. Step 3: partially unfolded SptP is guided through the EA for secretion [10,17,22,26,107]. Abbreviation: IM, inner membrane.

[4,10]. In fT3SS, secretion through the SctV homolog, FlhA, has been shown to be powered by the proton motive force [28,29]. Whether that is the case for vT3SS is not known.

Secretion regulation and timing

T3SS assembly and function are regulated. Designated σ-factors coordinate transcription of T3SS genes [6,12]. Substrate selection and secretion hierarchy are regulated by molecular switches [9]. Two switching mechanisms regulating secretion hierarchy are documented: early-to-middle substrates and middle-to-late substrates.

Secretion switching from early-to-middle substrates involves two steps: needle length measurement and substrate specificity switch facilitated by the ruler protein SctP and the EA component SctU, respectively [4,6,12]. SctP family ruler proteins are conserved and predicted to be unstructured. Various models are proposed for how SctP regulates needle length but no consensus has emerged [4,12]. Following needle assembly, SctU autocleavage switches secretion to that of the translocon proteins (middle substrates) in a mechanism that remains unclear [4,12,30]. Here, SepL (an SctW family protein; also termed gate keeper) bound to the protein SepD, interacts with SctV, thereby facilitating middle substrate secretion while preventing effector (late substrate) secretion [4,7,31]. The dissociation of SepL/SepD from SctV causes the apparatus to switch from middle to late substrate secretion [4,7,31]. The trigger for SepL/SepD disengagement from SctV remains unclear.

T4SS

T4SS machineries are large macromolecular machines capable of injecting DNAs and/or proteins [32–35]. Recently, Costa and Christie have introduced a classification of T4SSs into two

categories, the minimized and the expanded T4SSs, based on the number of components involved [36] (Figure S1B in the supplemental information online). Minimized T4SSs of gram-negative bacteria broadly consist of the 12 VirB1-11/VirD4 proteins (here we use the generally accepted VirB nomenclature initially derived from the *Agrobacterium* system). Expanded T4SSs are much larger, consisting of a greater number of components, for example, 32 for the *Legionella pneumophila* Dot/Icm T4SS [34,35]. In this review, we also use another classification based on function, which subdivides T4SSs into two functional classes: 'protein-injecting' T4SSs, mediating the secretion of proteins, and 'conjugative' T4SSs involved in DNA transfer, namely conjugation, which is the unidirectional transfer of DNAs from a donor cell to a recipient cell. Conjugative T4SS components are encoded by genes often located on plasmids. There is no overlap between the two types of classification: some conjugative T4SSs belong to the minimized class while others belong to the expanded class. The same is observed for protein-injecting T4SSs. It is also important to note that T4SSs mediating DNA transfer may also secrete proteins or protein–DNA complexes.

Diversity and nature of substrates

The principal substrate of conjugative T4SS systems is a nucleo-protein complex called the 'relaxosome'. However, prior to transferring DNA, conjugative T4SS must elaborate a pilus termed 'conjugative pilus' [37,38], a helical polymer of the VirB2 pilus subunit, which may serve in mediating interaction between donor and recipient cells or/and serve as a conduit for subsequent transfer of DNA. Therefore, conjugative T4SSs have an early substrate (the VirB2 pilus subunit) and a late substrate (the relaxosome) and they must be able to switch from early to late substrate secretion.

Early substrate VirB2 is a short IM-embedded two-transmembrane (TM) helix protein, which undergoes several maturation steps before being extracted from the IM to be assembled into a pilus [37].

Late substrate relaxosome is a complex composed of a main component, the relaxase, and a few accessory proteins, the number of which varies from one conjugative T4SS to another [39] (Figure 3A). The relaxase is a dual-function enzyme, with a trans-esterase domain at the N terminus and a helicase domain at the C terminus [40]. The relaxase specifically processes the plasmid DNA to be transferred by binding to a defined DNA sequence termed 'origin of transfer (*OriT*) DNA', nicking it on a single strand DNA (ssDNA) and covalently attaching to the resulting 5′-phosphate of the nicked strand [41]. Thus, the late substrate transferred by conjugative T4SSs is in fact an ssDNA–relaxase conjugate [42].

In contrast to conjugative T4SSs, protein-injecting T4SSs may not elaborate a pilus (defined as a polymer of pilus subunits) but may secrete one or many substrates that generally target multiple eukaryotic pathways. Substrates differ widely in their function, structure, cellular localization, and molecular properties [43]. Their number can vary greatly, from a single substrate (as is the case of the expanded *cag*-encoded T4SS from *Helicobacter pylori* [44]) to over 300 effector proteins (as is the case for the *dot/icm*-encoded T4SS from *L. pneumophila* [45]). For these systems, there is no distinction that has been made so far between early or late substrates.

Definition and description of the various SSs/sequences

The early substrate of conjugative T4SSs, VirB2, does not have an identifiable conserved SS but is distinctly hydrophobic, consisting of two TM helices [37].

In the late substrate relaxosome encoded by the F-family plasmids R1 and F (both encoding an expanded T4SS), three regions have been identified to be involved in recruitment: two domains

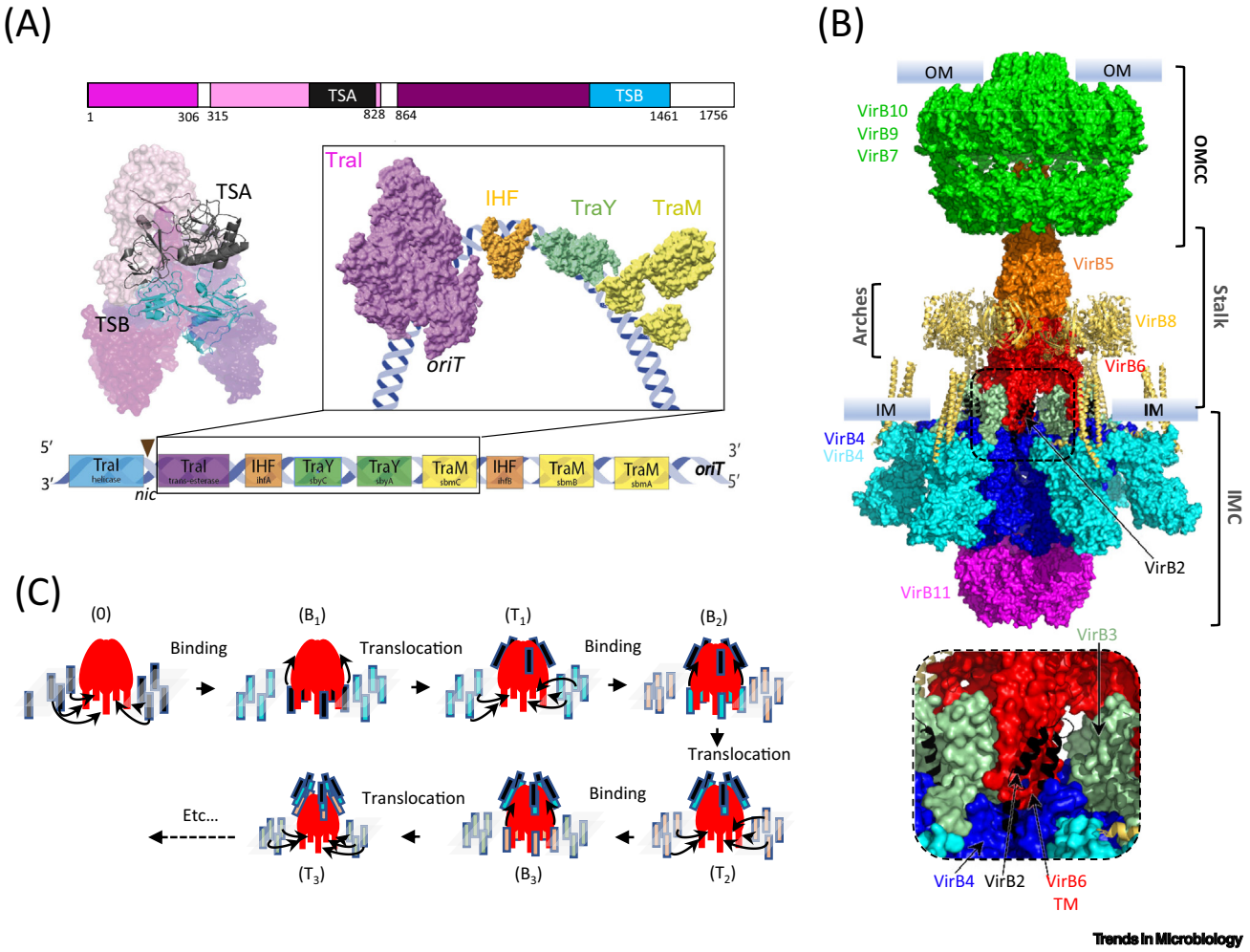

Figure 3. Conjugative type IV secretion system (T4SS): relaxosome, machinery, and mechanism of pilus biogenesis. (A) Late substrate relaxosome encoded by the F-plasmid. Top: domain organization of the TraI relaxase, color-coded magenta, pink, purple, black, and blue for the trans-esterase, vestigial helicase, active helicase, TSA, and TSB domains, respectively. Middle left: structure of the relaxase in surface representation, except for both TSA and TSB domains in ribbon, using the color-coding indicated above for each of the domains (PDB_5N8O [40]). Middle right: schematic diagram of the relaxosome containing the part of OriT DNA shown in rectangle in bottom panel, relaxase TraI, and the three accessory proteins TraM (PDB_3ON0 [48]), TraY (modeled using ROBETTA [110]), and IHF (PDB_1IHF [111]). Bottom: organization of *OriT* with the TraI (magenta), IHF (orange), TraM, (yellow), and TraY (green) binding sites. (B) Cryo-electron microscopy structure of the minimized conjugative T4SS machinery with early substrate VirB2 bound [56]. Upper panel: the T4SS components are shown in surface representation (PDB: 7O3J, 7O3T, 7O3V, 7O41, 7O42, 7O43, 7OIU, 7Q1V [56]), color-coded as indicated in labels. VirB2 (PDB_5LER [37]) is in black ribbon. The dashed line box surrounds the region magnified in bottom panel. (C) Mechanism of pilus biogenesis by conjugative T4SSs [56]. Three cycles of VirB2 subunit incorporation are shown. The VirB6 pentamer is shown as a dome-like red diagram with five legs [its transmembranes (TMs)]. The inner membrane (IM) is shown as semi-transparent lozenge and IM-embedded VirB2 subunits as vertical rectangles color-coded differently for each cycle. (0): unbound VirB6. (B_X): VirB2-bound state at the VirB6 TMs at cycle number x. T_x: translocated state where the VirB2s have been translocated to the assembly site at cycle number x. VirB2 translocation frees up the five VirB6 TMs so that five new subunits can be recruited. Each translocation step results in an additional layer of five VirB2 subunits inserting under the previously assembled layer at the assembly site. Abbreviations: IMC, inner membrane complex; OM, outer membrane; OMCC, outer membrane core complex.

in the relaxase TraI, TSA and TSB (for TS A and B) [46,47] and one in the accessory protein TraM [48] (Figure 3A).

In *L. pneumophila*, two effector groups have been identified: one where effectors depend for secretion on their interaction with the IcmSW chaperone complex (IcmSW-dependent effectors) [49] and another group that does not depend on that interaction (IcmSW-independent) [50].

IcmSW-binding sequences are scattered across the middle of effector sequences. Among the IcmSW-independent effectors, a subgroup was defined by the presence of a Glu-rich sequence at their ~30 C-terminal amino acid region [50,51]. In *Xanthomonas citri* (which encodes a minimized T4SS), secretion substrates carry a common ~100-residue Gln-rich motif near the C terminus, termed XVIPCDs (*Xanthomonas* VirD4-interacting protein conserved domain) [52]. In the human pathogen *Bartonella* spp. (also encoding a minimized T4SS), *Bartonella* effector proteins (Beps) contain a Bep intracellular delivery (BID) domain, a ~100-amino acid C terminus charged motif, that, together with a short positively charged C-terminal sequence, forms a bipartite T4SS signal [53,54]. In *H. pylori*, the CagA substrate contains a 20-residue SS at its C terminus and also a binding site for CagF [55].

Definition and description of the various recruitment platforms to which T4SS effectors bind

The recent cryo-EM structure of a minimized conjugative T4SS has identified a recruitment platform for early substrate VirB2 pilus subunits and a mechanism for their assembly into a pilus was proposed [56] (Figure 3B,C). Conjugative T4SSs are made of various subcomplexes (inner membrane complex, stalk, arches, and outer membrane core complex), as depicted in Figure 3B. The site of VirB2 recruitment was identified by coevolution and confirmed by site-directed mutagenesis as being the TM of one of the proteins present in the stalk, VirB6 [56]. VirB6 is a pentamer, not only acting as a recruitment platform for VirB2 in the IM, but, in addition, it contains a so-called 'assembly site' to which VirB2 subunits bound at the VirB6 TMs may be translocated to for pilus assembly in a mechanism detailed in Figure 3C [56].

For late substrate recruitment, conjugative T4SSs rely on a protein termed type 4 coupling protein (T4CP), which is an IM-anchored ATPase of the VirD4 family of proteins [34,57,58]. These ATPases usually function as ring-shape homo-hexamers that bind and hydrolyze nucleotides (Figure S2A in the supplemental information online). These ATPases are usually ~600 amino acids long, with some containing an additional extended C terminus, sometimes 200 residues long, that contains the interaction sites with other components [59,60]. For relaxosome recruitment, accessory protein TraM from the F plasmid has been shown to interact with T4CP TraD, the VirD4 homolog [61] (Figure S2B in the supplemental information online). TraM is a tetramer with an N-terminal ribbon-helix-helix (RHH) motif binding DNA and a C-terminal tetramerization domain [48]. Seven amino acids from the C-terminal extension of TraD interact with the tetramerization domain of TraM, suggesting a mechanism for relaxosome recruitment [61]. The target of TSA and TSB of the relaxase TraI is, however, unknown.

Protein-injecting expanded T4SSs generally utilize a type 4 coupling complex (T4CC) for substrate recruitment, the main component of which is also a VirD4-family ATPase. In the case of the *L. pneumophila* T4SS, VirD4-family ATPase DotL interacts with inner-membrane DotM, cytoplasmic DotN, and the cytoplasmic chaperones IcmSW [34]. Additional components include DotY and DotZ and sometimes LvgA [34] (Figure 4A). All interact like beads on a string with the extended C terminus of DotL. In *H. pylori*, the main ATPase Cagβ, stabilized by CagZ and assisted by accessory proteins CagF, also form a T4CC [44].

In *L. pneumophila*, we have described two effector groups, the IcmSW-dependent group and an IcmSW-independent group with C-terminal Glu-rich sequences. Correspondingly, these two groups interact with two distinct parts of the DotLMNYZ-IcmSW T4CC platform: one through the IcmSW module and one through DotM (Figure 4A) [51,62,63]. Interestingly, the IcmSW module can also bind LvgA, which participates in effector recruitment as well, although only a subset of IcmSW-dependent effectors are LvgA-dependent. LvgA binds at the middle of the U-shape IcmSW-DotL$_{C\text{-}ter}$ structure and functions as an adaptor for recruitment of LvgA-dependent

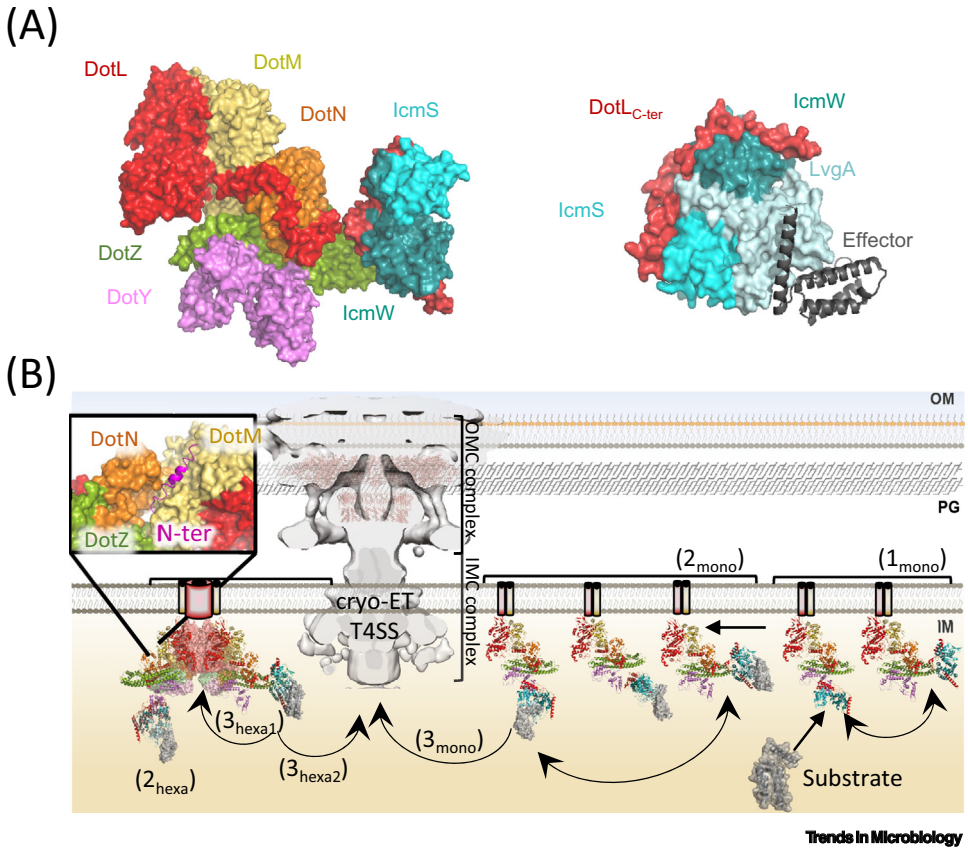

Figure 4. The *Legionella* type 4 coupling complex (T4CC) and model for effector recruitment by the expanded *Legionella pneumophila* type IV secretion system (T4SS). (A) The *Legionella* T4CC. Left panel: Cryo-electron microscopy structure (PDB_7OVB, EMD_10350, EMD_13083 [34,112]) of *L. pneumophila* T4CC in surface representation. Components are labeled and color-coded as in Figure S1B (see the supplemental information online). Right panel: crystal structure of DotL C-terminal sequence (DotL$_{C\text{-}ter}$) in complex with the chaperone module IcmSW, LvgA, and LvgA-dependent substrate VpdB (PDB 7BWK [64]). All proteins are in surface representation, except VpdB in ribbon, color coded red, teal/cyan, light blue, and dark grey for DotL$_{C\text{-}ter}$ (residues 656–783), IcmSW, accessory protein LvgA, and effector protein VpdB (residue 461–590), respectively. (B) Effector recruitment by the expanded *L. pneumophila* T4SS. Proteins are shown in ribbon and semi-transparent surface representation, except for structures in the box, which are shown in surface representation. Color-coding is as in (A). The T4CC may adopt two states, one where all of its seven components (DotLMNYZ-IcmSW) are present as monomers (monomeric T4CC) or another state where all components hexamerize via hexamerization of DotL/VirD4 (hexameric T4CC). State (1$_{mono}$): the IcmSW module bound to the DotL$_{C\text{-}ter}$ swings back and forth in the cytoplasm scanning for substrates. States (2$_{mono}$) and (2$_{hexa}$): IcmSW-mediated effector binding to monomeric T4CC or hexameric T4CC, respectively. Substrate is in grey surface. Step (3$_{mono}$) and (3$_{hexa1}$): swinging motion of the IcmSW module along a defined trajectory [112] brings substrates towards either the T4SS or the hexameric DotL channel. Step (3$_{hexa2}$): possible delivery to the T4SS from an hexameric T4CC. Zoomed in box shows the region of DotM, which binds IcmSW-independent substrates via their very acidic Glu-rich C-terminal signal (shown as pink ribbon). The cryo-electron tomography (cryo-ET) T4SS density is shown in grey and contoured at a σ level of 0.12 and 0.51 for the outer membrane complex (OMC) (EMD-7611) and inner membrane complex (IMC) (EMD-7612) maps, respectively [68]. Abbreviations: IM, inner membrane; OM, outer membrane, PG, peptidoglycan.

effectors [64] (Figure 4A). A recent crystal structure of the IcmSW-DotL-LvgA-effector complex, together with a previous study mapping effector binding to IcmSW, have suggested that recruitment to DotL might release the effector from the recruitment complex to the secretion channel [65]. For IcmSW-independent effectors with C-terminal Glu-rich signal sequences, the T4CC structure suggests that these SSs dock at the interface between DotM and DotN, where the

effector is likely to reside close to a small channel that connects to the main T4CC channel, thereby providing a route through the IM [34]. In *H. pylori*, Cagβ is required for recognition of the CagA translocation motif and guiding of CagA to the T4SS channel, probably in concert with its interaction partner CagZ [44].

Recruitment platforms in the context of the secretion machinery

The recruitment platform for early substrate VirB2 subunits, the stalk protein VirB6, is well characterized within the entire system (Figure 3B) [56]. On the periplasmic side, VirB6 is topped by the tip pilus subunit, VirB5. As layers of VirB2 subunits accumulate at the assembly site on VirB6, the VirB5 pentamer is pushed out at the tip of the growing pilus, eventually becoming exposed extracellularly. At its base in the IM, VirB6 interacts with the ATPase VirB4 (Figure 3B), which is thought to be the primary driver for pilus subunit translocation from their recruitment site to their assembly site.

The position of T4CP and T4CC proteins and complexes relative to the T4SS is still unclear. In the minimized conjugative T4SS encoded by the R388 plasmid, the T4CP, TrwB/VirD4, has been visualized sandwiched between two VirB4 hexameric barrels [66,67] (Figure S2A in the supplemental information online). This central position makes it ideal for secretion of the relaxase-ssDNA conjugate substrate. But the low resolution electron microscopy method used in this study has prevented further mechanistic insights.

In the case of *L. pneumophila*, cryo-ET studies have shown that while the secretion channel and the cytoplasmic ATPases are readily identified (Figure 4B), density that could be associated with the T4CC was not observed [68,69]. The high-resolution structure of the *Legionella* T4CC suggests that the complex might form its own channel through the IM [34]. However, several plausible mechanisms for effector delivery may be envisaged and are summarized in Figure 4B. In the case of *H. pylori*, *in situ* transmission electron microscopy (TEM) and mutagenesis have shown that the Cagβ/VirD4 protein is docked around the IM/cytoplasmic complex composed of CagE (the VirB4 homolog), Cagα (VirB11 homolog), and other unknown Cag subunits [70]. Waksman has suggested a potential interaction of VirB4-VirD4 in a hetero-hexameric configuration [33]; the *H. pylori* TEM structure supports this assumption and it is possible that the two proteins can only assemble upon host-induced activation.

Secretion regulation and timing

Very little mechanistic details are known about timing of secretion by T4SSs. In conjugative T4SS, the trigger for early to late substrate secretion switch is presumably the contact that the pilus makes with a recipient cell via unknown receptor–ligand interactions. This is followed by formation of the conjugative synapse, where the donor and recipient cells are brought in close contact [71], presumably leading to relaxosome assembly at the *OriT* site (although it is not excluded that the complex is preformed at this stage), docking of the relaxosome to the T4CP, and nicking of *OriT* prior to conjugate substrate transfer though the T4SS (Figure S2B in the supplemental information online). Bacterial signal-sensing systems such as quorum sensing (QS) and two-component (TC) systems participate in gene regulation and expression of the T4SS components and its substrates [72]. A new regulatory pathway of the *vir* regulon involving the bacterial secondary messenger cyclic di-guanosine monophosphate (cyclic-di-GMP) has been shown to play a role in *Legionella* and other bacteria T4SS regulation [73,74].

T6SS

The type VI secretion system (T6SS) is a protein secretion apparatus structurally and functionally similar to the phage injection machinery [75,76]. It is composed of three subcomplexes [the type six secretion X (TssX) nomenclature is here used for T6SS genes and proteins]: the membrane

complex comprising five copies of TssJLM proteins, connected to the baseplate made of six copies of TssKFGE proteins, attached to a tail tube-sheath with a spike. The tube-sheath is composed of hexameric layers of sheath proteins TssBC and tube hemolysin co-regulated (Hcp) protein, capped by a spike made of homotrimeric valine-glycine repeat G (VgrG) protein, itself tipped by a monomeric cone-shaped proline-alanine-alanine-arginine (PAAR) protein (Figure 5A and Figure S1C in the supplemental information online). Sheath contraction propels the VgrG-PAAR tip and Hcp tube through the baseplate and membrane complex and through the target cell envelope. Effectors loaded onto the tube-tip complex are then released, often leading to host cell death.

Diversity and nature of substrates

The T6SS effectors are subdivided into two groups, depending on their destination within target cells: the membrane/periplasm or the cytoplasm (reviewed in [77]). In brief, membrane/periplasmic acting effectors include, for example, type 6 lipase effector (Tle), which hydrolyzes phosphatidylethanolamine [78], type 6 membrane disrupting effectors (Tme) [79], or two other superfamilies of T6SS effectors [80,81] that cause cell lysis by degrading peptidoglycans. In the cytoplasmic acting effectors group, there is, for example, the type 6 DNase **e**ffector (Tde), which inhibits the growth of the target bacterial cells by degrading chromosomal DNA [82] or the DS-DNA Deaminases toxin A (DddA), which catalyzes the deamination of cytosine to uracil in double-stranded DNA (dsDNA) [83]. Most T6SS effectors are antimicrobial. Multiple effectors are usually delivered into target cells.

Definition and description of the various SSs/sequences

T6SS effectors do not contain linear SS sequences that facilitate their recognition by the T6SS apparatus [84]. To be secreted, effectors need to be translationally fused or bind (when encoded as separate genes) to the secreted T6SS core components PAAR, VgrG, or Hcp [77]. In both cases, interactions can be assisted by dedicated chaperones [85]. So far, a highly conserved prePAAR structural/sequence motif has been identified only in the PAAR-fused effector group (residues 6 to 15: AARxxDxxxH) (Figure 5B) [86]. This motif led to the identification of 6000 putative T6SS effectors, all of them possessing an N-terminal transmembrane domain (TMD) and co-occurring in genomes with an effector-associated gene (Eag) chaperone (Figure 5B; see also details later) [86]. Other sequences have been described but are specific of a unique type of interaction between one effector and one T6SS core component [87].

Definition and description of the various recruitment platforms to which these SSs bind

PARR, VgrG, and Hcp proteins act as T6SS recruitment platforms (Figure 5B–D) [77]. Most PAAR proteins consist of a ~100-amino acid sequence that folds into a cone-shaped structure (in salmon color in Figure 5A,B), the C terminus of which is exposed and may display an extension [88]. The latter may contain either an effector domain or a recruitment domain that meditates PAAR–effector interaction (Figure 5B) [88]. The VgrG spike protein forms a trimeric structure consisting of a cylinder-shaped base (gp27-like domain) followed by the small OB-fold domain surmounted by a β-helical prism extension named gp5 needle-like domain (in yellow in Figure 5A–C) [89,90]. Similar to PAAR, the gp5 needle domain can be followed by an additional C-terminal effector domain or effector-recruitment domain (Figure 5C) [91]. Hcp proteins form hexameric rings that are stacked to build an inner tube upon sheath formation [92]. The central channel of a Hcp ring has a diameter of roughly 40 Å, which can accommodate small, single-domain effectors that directly interact with Hcp (Figure 5D) [93]. Hcp may also contain an extension containing an effector domain but no effector-binding domain [94]. Additionally, Hcp also possesses chaperone-like properties that facilitate cytoplasmic accumulation of Hcp-interacting effectors prior to their secretion [93]. Membrane/periplasm effector group such as phospholipases are usually transported by VgrG proteins [78]. In contrast, cytoplasmic acting effectors are almost exclusively fused to PAAR and Hcp [95,96].

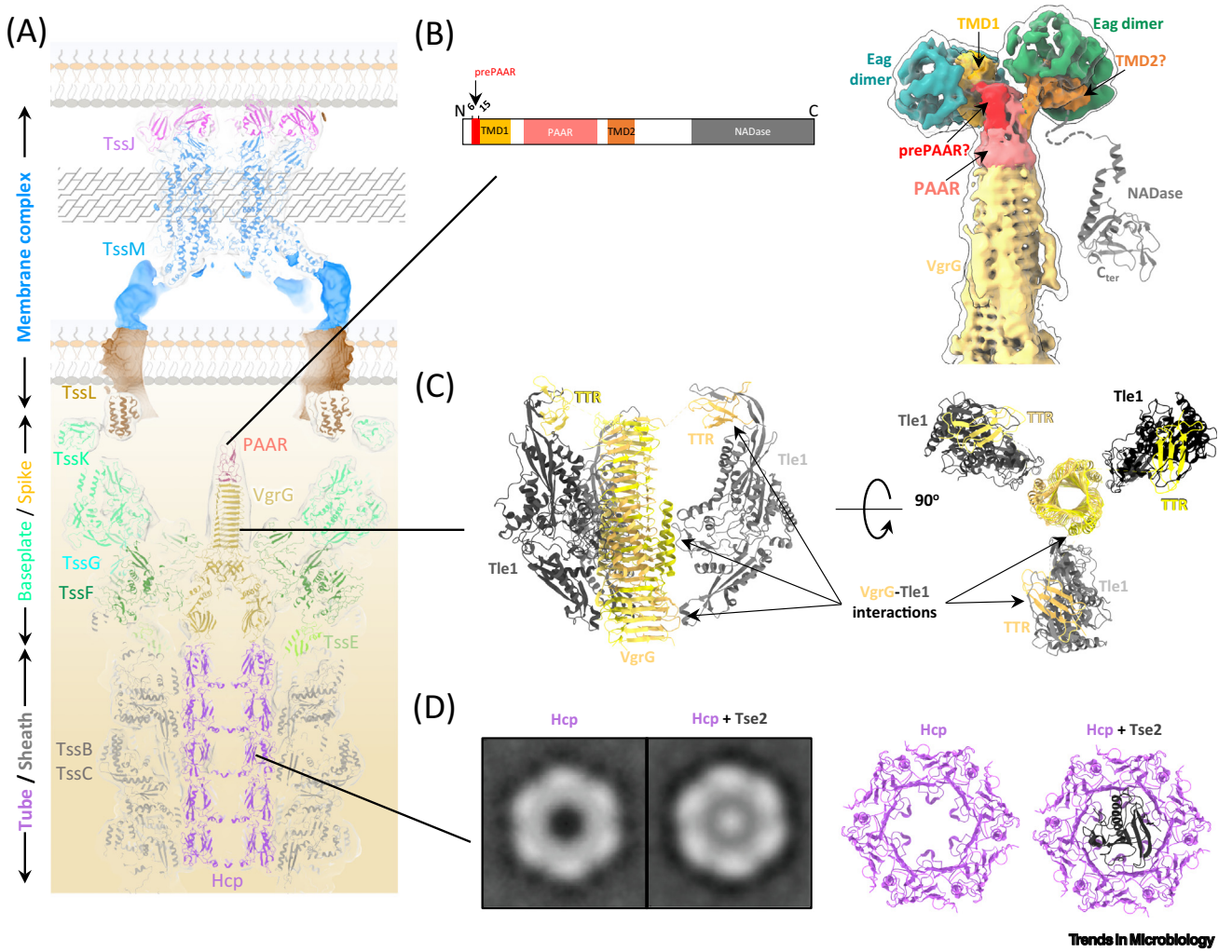

Figure 5. Type VI secretion system (T6SS): machinery, substrates, and substrate recruitment platforms. (A) Composite model of an assembled T6SS (gift of Remy Fronzes). Two cryo-electron tomography maps are shown in semi-transparent surface: for the membrane complex (EMD-0266 [113] (in grey except for parts of TssM (in blue) and TssL (in brown); contoured at 0.01 σ) and for the remaining of the T6SS (EMD-3879 [114] (in grey; contoured at 0.025 σ). Atomic resolution structures, shown in ribbon representation, are of the membrane complex (PDB-6HS7 [113]), the baseplate (PDB-6GIY, -6GJ3, -6GJ1 [115]), the Hcp/sheath (PDB-5MXN [92]), and the spike (PDB-4JIW for PAAR, PDB-2P5Z for VgrG [88,116]). (B) The PAAR effector-recruitment platform. Left: primary domain organization of *Pseudomonas aeruginosa* Tse6. Right: cryo-electron microscopy (cryo-EM) map of the *P. aeruginosa* VgrG/PAAR/Tse6 complex (EMD-0135 [98]; contoured at 0.03 σ) with various domains and proteins colored as in subpanel at left for Tse6, yellow for VgrG and cyan and green for the two Eag chaperone dimers. The positions of the two Eag dimers are shown as described in [98]. Those of TMD1 and prePAAR are from the crystal structure of the Eag/Tse6$_{NT}$ complex [86]. Also shown is a black ribbon representation of the crystal structure of the Tse6 NADase domain (PDB 4ZV4 [117]). Dashed line: flexible linker between the NADase domain and TMD2. (C) The VgrG effector-recruitment platform. Side (left) and top (right) views of the cryo-EM structure of the trimeric *Escherichia coli* VgrG-Tle1 complex (PDB 6SJL [99]), shown in yellow and black ribbon, respectively. The TTR domain extension of VgrG is labeled. (D) The Hcp effector recruitment platform. Two left subpanels: negative stain 2D class averages of the Hcp ring without (left) or with (right) the Tse2 effector. Two right subpanels: the Hcp structure (in purple) (PDB 5MXN [92]) with or without Tse2 effector (in black) (PDB 5AKO [118]). Tse2 was positioned manually inside the Hcp ring structure.

Molecular and structural basis of the interaction between SSs and recruitment platforms

Effectors covalently linked to VgrG or PAAR are generally composed of multiple domains and often require effector-specific chaperones. Thus far, three DUF chaperone families have been described: DUF1795, DUF2169, and DUF4123 [77]. The mechanism of DUF2169 and DUF4123 chaperones is unclear, however, they seem to facilitate the loading of a ternary

complex (chaperone/effector/PAAR) onto VgrG (Figure 6, step 1) [97]. In contrast, the mechanism of DUF1795 proteins, also known as Eag chaperones, is well characterized [86]. Eag chaperones interact and stabilize the TMD of the so-called 'evolved' PAAR proteins, which in a single polypeptide chain are composed of a PAAR domain, a prePAAR motif, one or two TMDs, and a C-terminal toxin domain (Figure 5B) [98]. The prePAAR motif is highly conserved and structurally complements a missing part of the PAAR domain (Figure 5B). Evolved PAAR proteins are classified into two classes (see PAAR pathway in Figure 6) [86]. Class I effectors belong to the Rhs family of proteins, are comprised of ~1200 amino acids, and possess a single TMD. Class II effectors are ~450 amino acids in length, contain two N-terminal TMDs, and a GxxxxGxxLxGxxxD motif. TMDs-Eag and prePAAR-PAAR interactions are required for VgrG interaction and effector stability, presumably by masking the TMDs.

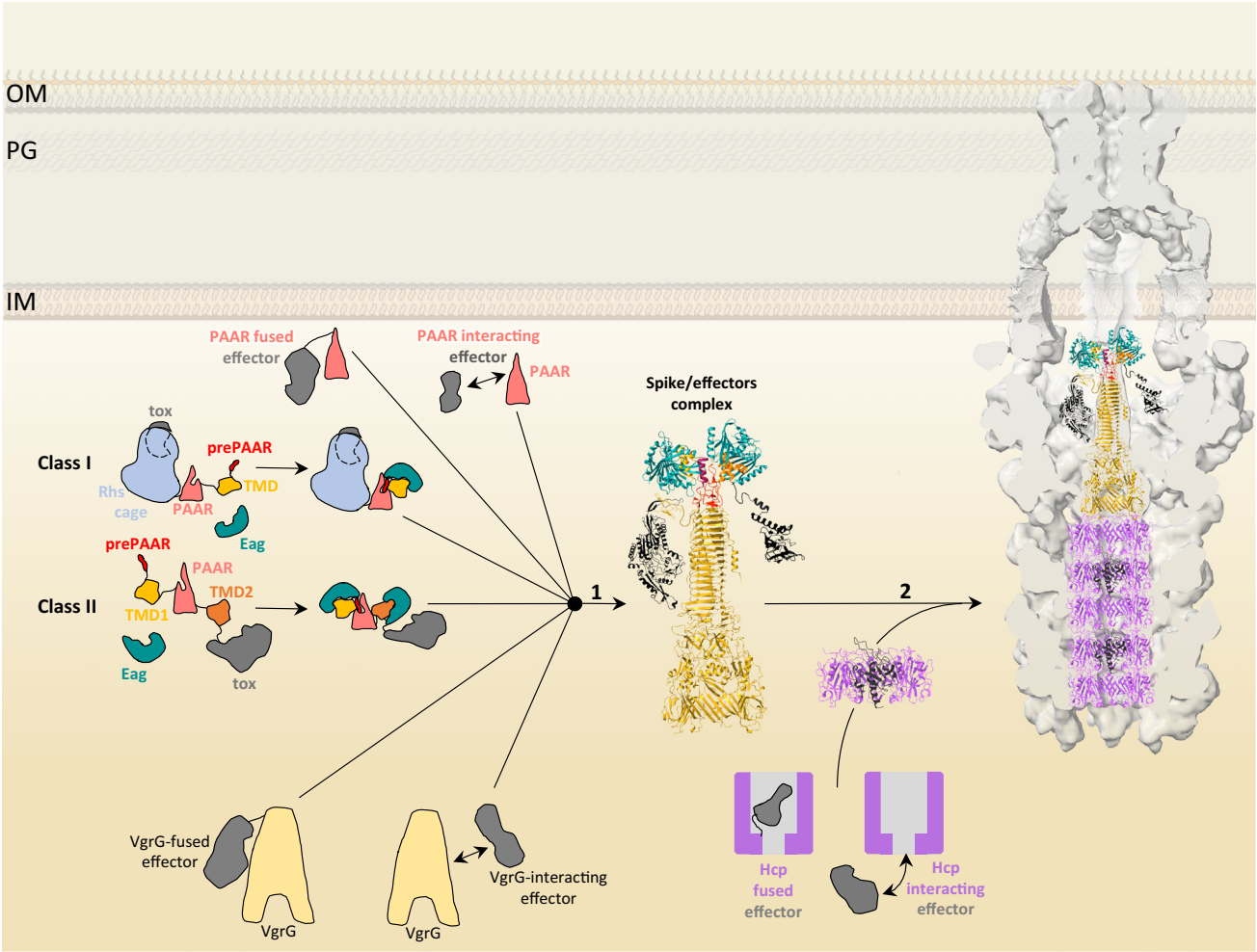

Figure 6. Model for effectors recruitment by type VI secretion system (T6SS). T6SS effectors are recruited to the machinery through assembly of recruitment platforms VgrG, PAAR, and Hcp during which various combinations of effectors are selected. Recruitment steps are therefore intimately coupled to assembly steps in the manner described here. Step 1: various PAARs and VgrGs either covalently or noncovalently bound to effectors combine competitively to form a unique set of spike-loaded effectors. Step 2: Hcp-bound effectors are next recruited during Hcp tube formation, leading to a fully loaded T6SS. All recruitment platforms are labeled. Color-coding for the rest of the machinery (sheath, base plate, and membrane complex) is as in Figure 5A.

As mentioned earlier, effectors may interact noncovalently with C-terminal extension regions of VgrG/PAAR proteins that form effector-binding domains. An example of such a domain is Transthyretin-like domain (TTR) [99]. The structure of VgrG-TTR bound to three Tle1 effectors was solved by cryo-EM (Figure 5C), showing an extensive interface, a region of which was shown to inhibit Tle1 phospholipase activity [99]. Finally, individual Hcp rings display affinity toward multiple unrelated effectors [100]. However, the molecular basis for this promiscuous substrate recognition is unknown. Moreover, some effectors fused to Hcp have been identified [94].

Secretion regulation and timing

Crucial to the fate of an effector is its assembly within the Hcp tube and spike complex (Figure 6). VgrG, PAAR, and Hcp proteins (with their covalently or noncovalently bound effectors) may compete with each other and their assembly may result in various combinations of effector functions being injected into target cells, as illustrated in Figure 6 [101]. Secondly, tight transcriptional, post-transcriptional, and post-translational control (including phosphorylation) has been observed [102,103]. Some common trends in regulatory mechanisms of T6SS include QS, changes in temperature and pH, and TC regulatory systems. Although some T6SSs in some bacterial species are tightly regulated, other species or strains exhibit constitutively active T6SSs. Ultimately, T6SS firing is triggered by contact with a target cell. Some bacteria, like *Pseudomonas aeruginosa*, activate the T6SS solely as a defensive weapon, while other species, such as *Proteus mirabilis* and *Serratia marcescens*, do not require an attack by neighboring cells to fire the T6SS [104].

Concluding remarks

All bacterial injectisomes must include substrate recruitment platforms, the crucial role of which is to provide optimal location and priming for subsequent secretion. These platforms are extremely varied, either being composed of one protein (T4CP for minimized T4SSs or VgrG, PARR, or Hcp for T6SSs) or forming large complexes such as for T3SSs or expanded T4SSs. Within these larger complex frameworks, they may form cage-like structures (T3SSs) or more compact structures (T4SSs). In turn, their great diversity in shape and composition mirrors equally diverse recruitment and secretion mechanisms, sometimes requiring chaperone-mediated unfolding (T3SS and expanded T4SS), sometimes not (conjugative T4SS early and late substrates and some T6SS effectors).

Substrate recruitment also follows various modalities, ranging from covalent binding to parts of the core secretion machinery in the case of some T6SS substrates, to noncovalent binding of effectors to various components of the cognate recruitment platform. In the case of T3SS (effectors) and conjugative T4SS (late substrate), coupling ATPases play crucial roles in serving as direct recruitment platforms, which affords direct coupling between ATP binding/hydrolysis and secretion. However, in some other examples, such as T6SS effectors, the only known ATPase (ClpV) hardly plays a direct role in effector recruitment, being instead involved in tube and sheath disassembly. In expanded protein-injecting T4SS, various families of effectors appear to target various components of the T4CC (IcmSW, DotM, and possibly others) but the role of its ATPase component (DotL) is unclear.

A recurrent theme in substrate recruitment is the essential role that chaperones play. Chaperones generally prime substrates for secretion by maintaining them in a partially unfolded state, thereby affording the passage of substrates through narrow secretion channels, and/or by lowering the energetic barrier for secretion. As a result, the substrate is often recruited in a chaperone-bound state. This has been ubiquitously observed, except in conjugative T4SSs where no chaperone has been identified for any of the two main substrates, the early substrate VirB2

Outstanding questions

T3SS:

- What is the molecular basis for secretion signal and translocation signal recognition by the sorting complex?
- What is the mechanism of early-to-middle and middle-to-late substrate switches?
- How does the sorting complex ATPase work in capturing substrates and handing them over to the export apparatus?
- What is the mechanism of chaperone release prior or during secretion?

Conjugative T4SS:

- What is the mechanism of recipient cell recognition by donor cells?
- What is the molecular basis of DNA processing by the relaxosome?
- What is the molecular basis of relaxosome recruitment by the type 4 coupling protein?
- What is the pathway of relaxase–ssDNA transport from donor to the recipient cell and what is the role of the pilus?
- What is the DNA-transport channel in the recipient cell?

Expanded protein-injecting T4SS:

- What is the mechanism of IcmSW-independent effector recruitment?
- What is the molecular basis for substrate release?
- How does the type 4 coupling complex and T4SS connect and how are substrates handed over between the two complexes?
- Has type 4 coupling complex modularity been fully explored; in other words, are there other DotYZ-like proteins affecting type 4 coupling complex function?

T6SS:

- How are effectors selected for secretion? Or is 'selection' a random combinatorial process occurring during T6SS assembly?
- What is the role of T6SS chaperones in priming effectors for assembly into

or the late substrate relaxosome. It could be that it is yet to be discovered, or there just may be no need for it. Indeed, for VirB2, it has been shown that in its final assembly state, that of a pilus, a phospholipid is being incorporated stoichiometrically together with the subunit, thereby lowering the energetic barrier for subunit extraction from the IM. For the late substrate relaxosome, it has been shown that the actual substrate to be transported is an ssDNA–protein conjugate in which the proteinaceous component of the conjugate, the relaxase, can be easily unfolded [105] and the DNA component easily melted into a single strand through the action of a helicase [40].

Although many aspects of their mechanism remain to be investigated (see Outstanding questions), substrate-recruitment platforms ought to be key targets for the design of molecules capable of inhibiting effector secretion by bacterial pathogens. However, until now, the paucity of structural information on recruitment frameworks has prevented the field from focusing on such an endeavor. This is now changing rapidly as molecular interaction details on substrate recruitment are being unraveled. Because there is a diverse array of recruitment mechanisms, there is hope that specificity can be achieved, inhibiting virulence in a targeted fashion. Also, a better understanding of effector recruitment mechanism might allow the design of novel delivery systems engineered to inject therapeutic molecules in humans, animals, and plants, as well as novel antimicrobials.

the T6SS machinery and subsequent secretion?
- What is the mechanism of effector loading onto the secretion machinery?
- After spring loading of the sheath, how do cell contacts trigger firing of the machinery?

Declaration of interests

No interests are declared.

Supplemental information

Supplemental information associated with this article can be found online at https://doi.org/10.1016/j.tim.2023.03.005.

References

1. Costa, T.R. *et al.* (2015) Secretion systems in gram-negative bacteria: structural and mechanistic insights. *Nat. Rev. Microbiol.* 13, 343–359
2. Galan, J.E. and Waksman, G. (2018) Protein-injection machines in bacteria. *Cell* 172, 1306–1318
3. Rego, A.T. *et al.* (2010) Two-step and one-step secretion mechanisms in gram-negative bacteria: contrasting the type IV secretion system and the chaperone-usher pathway of pilus biogenesis. *Biochem. J.* 425, 475–488
4. Deng, W. *et al.* (2017) Assembly, structure, function and regulation of type III secretion systems. *Nat. Rev. Microbiol.* 15, 323–337
5. Erhardt, M. *et al.* (2014) ATPase-independent type-III protein secretion in *Salmonella enterica*. *PLoS Genet.* 10, e1004800
6. Portaliou, A.G. *et al.* (2016) Type III secretion: building and operating a remarkable nanomachine. *Trends Biochem. Sci.* 41, 175–189
7. Portaliou, A.G. *et al.* (2017) Hierarchical protein targeting and secretion is controlled by an affinity switch in the type III secretion system of enteropathogenic *Escherichia coli*. *EMBO J.* 36, 3517–3531
8. Deng, W. *et al.* (2015) SepD/SepL-dependent secretion signals of the type III secretion system translocator proteins in enteropathogenic *Escherichia coli*. *J. Bacteriol.* 197, 1263–1275
9. Lilic, M. *et al.* (2006) A common structural motif in the binding of virulence factors to bacterial secretion chaperones. *Mol. Cell* 21, 653–664
10. Majewski, D.D. *et al.* (2019) Cryo-EM structure of the homohexameric T3SS ATPase-central stalk complex reveals rotary ATPase-like asymmetry. *Nat. Commun.* 10, 626
11. Munera, D. *et al.* (2010) N-terminal type III secretion signal of enteropathogenic *Escherichia coli* translocator proteins. *J. Bacteriol.* 192, 3534–3539
12. Deane, J.E. *et al.* (2010) Timing is everything: the regulation of type III secretion. *Cell. Mol. Life Sci.* 67, 1065–1075
13. Butan, C. *et al.* (2019) High-resolution view of the type III secretion export apparatus *in situ* reveals membrane remodeling and a secretion pathway. *Proc. Natl. Acad. Sci. U. S. A.* 116, 24786–24795
14. Akeda, Y. and Galán, J.E. (2005) Chaperone release and unfolding of substrates in type III secretion. *Nature* 437, 911–915
15. Lee, S.H. and Galán, J.E. (2004) *Salmonella* type III secretion-associated chaperones confer secretion-pathway specificity. *Mol. Microbiol.* 51, 483–495
16. Tomalka, A.G. *et al.* (2012) A translocator-specific export signal establishes the translocator–effector secretion hierarchy that is important for type III secretion system function. *Mol. Microbiol.* 86, 1464–1481
17. Stebbins, C.E. and Galán, J.E. (2001) Maintenance of an unfolded polypeptide by a cognate chaperone in bacterial type III secretion. *Nature* 414, 77–81
18. Luo, Y. *et al.* (2001) Structural and biochemical characterization of the type III secretion chaperones CesT and SigE. *Nat. Struct. Biol.* 8, 1031–1036
19. Yip, C.K. *et al.* (2005) Structural characterization of a type III secretion system filament protein in complex with its chaperone. *Nat. Struct. Mol. Biol.* 12, 75–81
20. Chen, L. *et al.* (2013) Substrate-activated conformational switch on chaperones encodes a targeting signal in type III secretion. *Cell Rep.* 3, 709–715
21. Lara-Tejero, M. *et al.* (2011) A sorting platform determines the order of protein secretion in bacterial type III systems. *Science* 331, 1188–1191
22. Hu, B. *et al.* (2017) *In situ* molecular architecture of the *Salmonella* type III secretion machine. *Cell* 168, 1065–1074
23. Hu, B. *et al.* (2015) Visualization of the type III secretion sorting platform of *Shigella flexneri*. *Proc. Natl. Acad. Sci. U. S. A.* 112, 1047–1052

24. Miletic, S. *et al.* (2021) Substrate-engaged type III secretion system structures reveal gating mechanism for unfolded protein translocation. *Nat. Commun.* 12, 1546
25. Johnson, S. *et al.* (2019) The structure of an injectisome export gate demonstrates conservation of architecture in the core export gate between flagellar and virulence type III secretion systems. *mBio* 10, e00818–19
26. Allison, S.E. *et al.* (2014) Identification of the docking site between a type III secretion system ATPase and a chaperone for effector cargo. *J. Biol. Chem.* 289, 23734–23744
27. Gilzer, D. *et al.* (2022) Direct interaction of a chaperone-bound type III secretion substrate with the export gate. *Nat. Commun.* 13, 2858
28. Minamino, T. and Namba, K. (2008) Distinct roles of the FliI ATPase and proton motive force in bacterial flagellar protein export. *Nature* 451, 485–488
29. Paul, K. *et al.* (2008) Energy source of flagellar typeIII secretion. *Nature* 451, 489–492
30. Zarivach, R. *et al.* (2008) Structural analysis of the essential self-cleaving type III secretion proteins EscU and SpaS. *Nature* 453, 124–127
31. Burkinshaw, B.J. *et al.* (2015) Structural analysis of SepL, an enteropathogenic *Escherichia coli* type III secretion-system gatekeeper protein. *Acta Crystallogr. Sect. F* 71, 1300–1308
32. Grohmann, E. *et al.* (2018) Type IV secretion in gram-negative and gram-positive bacteria. *Mol. Microbiol.* 107, 455–471
33. Waksman, G. (2019) From conjugation to T4S systems in gram-negative bacteria: a mechanistic biology perspective. *EMBO Rep.* 20, e47012
34. Meir, A. *et al.* (2020) Mechanism of effector capture and delivery by the type IV secretion system from *Legionella pneumophila*. *Nat. Commun.* 11, 2864
35. Sheedlo, M.J. *et al.* (2021) Cryo-EM reveals new species-specific proteins and symmetry elements in the *Legionella pneumophila* Dot/Icm T4SS. *Elife* 10, e70427
36. Costa, T.R.D. *et al.* (2021) Type IV secretion systems: advances in structure, function, and activation. *Mol. Microbiol.* 115, 436–452
37. Costa, T.R.D. *et al.* (2016) Structure of the bacterial sex F pilus reveals an assembly of a stoichiometric protein-phospholipid complex. *Cell* 166, 1436–1444
38. Ripoll-Rozada, J. *et al.* (2013) Functional interactions of VirB11 traffic ATPases with VirB4 and VirD4 molecular motors in type IV secretion systems. *J. Bacteriol.* 195, 4195–4201
39. de la Cruz, F. *et al.* (2010) Conjugative DNA metabolism in gram-negative bacteria. *FEMS Microbiol. Rev.* 34, 18–40
40. Ilangovan, A. *et al.* (2017) Cryo-EM structure of a relaxase reveals the molecular basis of DNA unwinding during bacterial conjugation. *Cell* 169, 708–721
41. Fu, Y.H. *et al.* (1991) Deletion analysis of the F plasmid oriT locus. *J. Bacteriol.* 173, 1012–1020
42. Wong, J.J. *et al.* (2012) Relaxosome function and conjugation regulation in F-like plasmids - a structural biology perspective. *Mol. Microbiol.* 85, 602–617
43. Li, Y.G. *et al.* (2019) Biological and structural diversity of type IV secretion systems. *Microbiol. Spectr.* 7, 1128
44. Cover, T.L. *et al.* (2020) The *Helicobacter pylori* Cag type IV secretion system. *Trends Microbiol.* 28, 682–695
45. Gomez-Valero, L. *et al.* (2019) More than 18,000 effectors in the *Legionella* genus genome provide multiple, independent combinations for replication in human cells. *Proc. Natl. Acad. Sci. U. S. A.* 116, 2265–2273
46. Lang, S. *et al.* (2010) Molecular recognition determinants for type IV secretion of diverse families of conjugative relaxases. *Mol. Microbiol.* 78, 1539–1555
47. Redzej, A. *et al.* (2013) Structure of a translocation signal domain mediating conjugative transfer by type IV secretion systems. *Mol. Microbiol.* 89, 324–333
48. Wong, J.J. *et al.* (2011) Structural basis of cooperative DNA recognition by the plasmid conjugation factor, TraM. *Nucleic Acids Res.* 39, 6775–6788
49. Jeong, K.C. *et al.* (2015) Novel export control of a *Legionella* Dot/Icm substrate is mediated by dual, independent signal sequences. *Mol. Microbiol.* 96, 175–188
50. Lifshitz, Z. *et al.* (2013) Computational modeling and experimental validation of the *Legionella* and *Coxiella* virulence-related type-IVB secretion signal. *Proc. Natl. Acad. Sci. U. S. A.* 110, E707–E715
51. Meir, A. *et al.* (2018) *Legionella* DotM structure reveals a role in effector recruiting to the type 4B secretion system. *Nat. Commun.* 9, 507
52. Alegria, M.C. *et al.* (2005) Identification of new protein-protein interactions involving the products of the chromosome- and plasmid-encoded type IV secretion loci of the phytopathogen *Xanthomonas axonopodis pv. citri*. *J. Bacteriol.* 187, 2315–2325
53. Schulein, R. *et al.* (2005) A bipartite signal mediates the transfer of type IV secretion substrates of *Bartonella henselae* into human cells. *Proc. Natl. Acad. Sci. U. S. A.* 102, 856–861
54. Wagner, A. *et al.* (2019) Versatility of the BID domain: conserved function as type IV secretion signal and secondarily evolved effector functions within *Bartonella* infected host cells. *Front. Microbiol.* 10, 921
55. Schindele, F. *et al.* (2016) Quantitative analysis of CagA type IV secretion by *Helicobacter pylori* reveals substrate recognition and translocation requirements. *Mol. Microbiol.* 100, 188–203
56. Macé, K. *et al.* (2022) Cryo-EM structure of a type IV secretion system. *Nature* 607, 191–196
57. Schröder, G. *et al.* (2002) TraG-like proteins of DNA transfer systems and of the *Helicobacter pylori* type IV secretion system: inner membrane gate for exported substrates? *J. Bacteriol.* 184, 2767–2779
58. Gomis-Rüth, F.X. *et al.* (2001) The bacterial conjugation protein TrwB resembles ring helicases and F1-ATPase. *Nature* 409, 637–641
59. Lee, M.H. *et al.* (1999) Analysis of F factor TraD membrane topology by use of gene fusions and trypsin-sensitive insertions. *J. Bacteriol.* 181, 6108–6113
60. Disqué-Kochem, C. and Dreiseikelmann, B. (1997) The cytoplasmic DNA-binding protein TraM binds to the inner membrane protein TraD *in vitro*. *J. Bacteriol.* 179, 6133–6137
61. Lu, J. *et al.* (2008) Structural basis of specific TraD-TraM recognition during F plasmid-mediated bacterial conjugation. *Mol. Microbiol.* 70, 89–99
62. Ninio, S. *et al.* (2005) The *Legionella* IcmS-IcmW protein complex is important for Dot/Icm-mediated protein translocation. *Mol. Microbiol.* 55, 912–926
63. Cambronne, E.D. and Roy, C.R. (2007) The *Legionella pneumophila* IcmSW complex interacts with multiple Dot/Icm effectors to facilitate type IV translocation. *PLoS Pathog.* 3, e188
64. Kim, H. *et al.* (2020) Structural basis for effector protein recognition by the Dot/Icm type IVB coupling protein complex. *Nat. Commun.* 11, 2623
65. Xu, J. *et al.* (2017) Structural insights into the roles of the IcmS-IcmW complex in the type IVb secretion system of *Legionella pneumophila*. *Proc. Natl. Acad. Sci. U. S. A.* 114, 13543–13548
66. Low, H.H. *et al.* (2014) Structure of a type IV secretion system. *Nature* 508, 550–553
67. Redzej, A. *et al.* (2017) Structure of a VirD4 coupling protein bound to a VirB type IV secretion machinery. *EMBO J.* 36, 3080–3095
68. Chetrit, D. *et al.* (2018) A unique cytoplasmic ATPase complex defines the *Legionella pneumophila* type IV secretion channel. *Nat. Microbiol.* 3, 678–686
69. Ghosal, D. *et al.* (2017) In situ structure of the *Legionella* Dot/Icm type IV secretion system by electron cryotomography. *EMBO Rep.* 18, 726–732
70. Hu, B. *et al.* (2019) *In situ* molecular architecture of the *Helicobacter pylori* Cag type IV secretion system. *mBio* 10, e00849-19
71. Low, W.W. *et al.* (2022) Mating pair stabilization mediates bacterial conjugation species specificity. *Nat. Microbiol.* 7, 1016–1027
72. Pena, R.T. *et al.* (2019) Relationship between quorum sensing and secretion systems. *Front. Microbiol.* 10, 1100

73. Allombert, J. *et al.* (2021) Deciphering *Legionella* effector delivery by Icm/Dot secretion system reveals a new role for c-di-GMP signaling. *J. Mol. Biol.* 433, 166985
74. McCarthy, R.R. *et al.* (2019) Cyclic di-GMP inactivates T6SS and T4SS activity in *Agrobacterium tumefaciens*. *Mol. Microbiol.* 112, 632–648
75. Wang, J. *et al.* (2019) Assembly and subcellular localization of bacterial type VI secretion systems. *Annu. Rev. Microbiol.* 73, 621–638
76. Cascales, E. and Cambillau, C. (2012) Structural biology of type VI secretion systems. *Philos. Trans. R. Soc. Lond. Ser. B Biol. Sci.* 367, 1102–1111
77. Jurėnas, D. and Journet, L. (2021) Activity, delivery, and diversity of type VI secretion effectors. *Mol. Microbiol.* 115, 383–394
78. Russell, A.B. *et al.* (2013) Diverse type VI secretion phospholipases are functionally plastic antibacterial effectors. *Nature* 496, 508–512
79. Mariano, G. *et al.* (2019) A family of type VI secretion system effector proteins that form ion-selective pores. *Nat. Commun.* 10, 1–15
80. Russell, A.B. *et al.* (2011) Type VI secretion delivers bacteriolytic effectors to target cells. *Nature* 475, 343–347
81. Whitney, J.C. *et al.* (2013) Identification, structure, and function of a novel type VI secretion peptidoglycan glycoside hydrolase effector-immunity pair. *J. Biol. Chem.* 288, 26616–26624
82. Pissaridou, P. *et al.* (2018) The *Pseudomonas aeruginosa* T6SS-VgrG1b spike is topped by a PAAR protein eliciting DNA damage to bacterial competitors. *Proc. Natl. Acad. Sci. U. S. A.* 115, 12519–12524
83. Mok, B.Y. *et al.* (2020) A bacterial cytidine deaminase toxin enables CRISPR-free mitochondrial base editing. *Nature* 583, 631–637
84. An, Y. *et al.* (2018) Comprehensive assessment and performance improvement of effector protein predictors for bacterial secretion systems III, IV and VI. *Brief. Bioinform.* 19, 148–161
85. Unterweger, D. *et al.* (2017) Adaptor proteins of type VI secretion system effectors. *Trends Microbiol.* 25, 8–10
86. Ahmad, S. *et al.* (2020) Structural basis for effector transmembrane domain recognition by type VI secretion system chaperones. *eLife* 9, 1–29
87. Burkinshaw, B.J. *et al.* (2018) (2018) A type VI secretion system effector delivery mechanism dependent on PAAR and a chaperone–co-chaperone complex. *Nat. Microbiol.* 3, 632–640
88. Shneider, M.M. *et al.* (2013) PAAR-repeat proteins sharpen and diversify the type VI secretion system spike. *Nature* 500, 350–353
89. Spínola-Amilibia, M. *et al.* (2016) The structure of VgrG1 from *Pseudomonas aeruginosa*, the needle tip of the bacterial type VI secretion system. *Acta Crystallogr. D Struct. Biol.* 72, 22–33
90. Uchida, K. *et al.* (2014) Structure and properties of the C-terminal β-helical domain of VgrG protein from *Escherichia coli* O157. *J. Biochem.* 155, 173–182
91. Flaugnatti, N. *et al.* (2016) A phospholipase A1 antibacterial type VI secretion effector interacts directly with the C-terminal domain of the VgrG spike protein for delivery. *Mol. Microbiol.* 99, 1099–1118
92. Wang, J. *et al.* (2017) Cryo-EM structure of the extended type VI secretion system sheath-tube complex. *Nat. Microbiol.* 2, 1507–1512
93. Silverman, J.M. *et al.* (2013) Haemolysin coregulated protein is an exported receptor and chaperone of type VI secretion substrates. *Mol. Cell* 51, 584–593
94. Ma, J. *et al.* (2017) The Hcp proteins fused with diverse extended-toxin domains represent a novel pattern of antibacterial effectors in type VI secretion systems. *Virulence* 8, 1189–1202
95. Jana, B. *et al.* (2019) A modular effector with a DNase domain and a marker for T6SS substrates. *Nat. Commun.* 10, 1–12
96. Koskiniemi, S. *et al.* (2013) Rhs proteins from diverse bacteria mediate intercellular competition. *Proc. Natl. Acad. Sci. U. S. A.* 110, 7032–7037
97. Bondage, D.D. *et al.* (2016) VgrG C terminus confers the type VI effector transport specificity and is required for binding with PAAR and adaptor–effector complex. *Proc. Natl. Acad. Sci. U. S. A.* 113, E3931–E3940
98. Quentin, D. *et al.* (2018) (2018) Mechanism of loading and translocation of type VI secretion system effector Tse6. *Nat. Microbiol.* 3, 1142–1152
99. Flaugnatti, N. *et al.* (2020) Structural basis for loading and inhibition of a bacterial T6SS phospholipase effector by the VgrG spike. *EMBO J.* 39, e104129
100. Whitney, J.C. *et al.* (2014) Genetically distinct pathways guide effector export through the type VI secretion system. *Mol. Microbiol.* 92, 529–542
101. Jana, B. and Salomon, D. (2019) Type VI secretion system: a modular toolkit for bacterial dominance. *Future Microbiol.* 14, 1451–1463
102. Mougous, J.D. *et al.* (2007) (2007) Threonine phosphorylation post-translationally regulates protein secretion in *Pseudomonas aeruginosa*. *Nat. Cell Biol.* 9, 797–803
103. Miyata, S.T. *et al.* (2013) Type VI secretion system regulation as a consequence of evolutionary pressure. *J. Med. Microbiol.* 62, 663–676
104. Ostrowski, A. *et al.* (2018) Killing with proficiency: integrated post-translational regulation of an offensive type VI secretion system. *PLoS Pathog.* 14, e1007230
105. Trokter, M. and Waksman, G. (2018) Translocation through the conjugative type IV secretion system requires unfolding of its protein substrate. *J. Bacteriol.* 200, e00615–e00617
106. Kuhlen, L. *et al.* (2020) The substrate specificity switch FlhB assembles onto the export gate to regulate type three secretion. *Nat. Commun.* 11, 1296
107. Abrusci, P. *et al.* (2013) Architecture of the major component of the type III secretion system export apparatus. *Nat. Struct. Mol. Biol.* 20, 99–104
108. Sun, P. *et al.* (2008) Structural characterization of the *Yersinia pestis* type III secretion system needle protein YscF in complex with its heterodimeric chaperone YscE/YscG. *J. Mol. Biol.* 377, 819–830
109. Lunelli, M. *et al.* (2009) IpaB-IpgC interaction defines binding motif for type III secretion translocator. *Proc. Natl. Acad. Sci. U. S. A.* 106, 9661–9666
110. Yang, J. *et al.* (2020) Improved protein structure prediction using predicted interresidue orientations. *Proc. Natl. Acad. Sci. U. S. A.* 117, 1496–1503
111. Rice, P.A. *et al.* (1996) Crystal structure of an IHF-DNA complex: a protein-induced DNA U-turn. *Cell* 87, 1295–1306
112. Mace, K. *et al.* (2022) Proteins DotY and DotZ modulate the dynamics and localization of the type IVB coupling complex of *Legionella pneumophila*. *Mol. Microbiol.* 117, 307–319
113. Rapisarda, C. *et al.* (2019) *In situ* and high-resolution cryo-EM structure of a bacterial type VI secretion system membrane complex. *EMBO J.* 38, e100886
114. Nazarov, S. *et al.* (2018) Cryo-EM reconstruction of type VI secretion system baseplate and sheath distal end. *EMBO J.* 37, e97103
115. Cherrak, Y. *et al.* (2018) Biogenesis and structure of a type VI secretion baseplate. *Nat. Microbiol.* 3, 1404–1416
116. Leiman, P.G. *et al.* (2009) Type VI secretion apparatus and phage tail-associated protein complexes share a common evolutionary origin. *Proc. Natl. Acad. Sci. U. S. A.* 106, 4154–4159
117. Whitney, J.C. *et al.* (2015) An interbacterial NAD(P)+ glycohydrolase toxin requires elongation factor Tu for delivery to target cells. *Cell* 163, 607–619
118. Robb, C.S. *et al.* (2016) The structure of the toxin and type 6 secretion system substrate Tse2 in complex with its immunity protein. *Structure* 24, 277–284